ARMY RESEARCH LABORATORY

Comparison of MBT and BTQB Quantum Well Infrared Photodetectors and Implications for Multicolor Design

Stephen W. Kennerly, Daniel W. Beekman, John W. Little,
Arnold C. Goldberg, Richard P. Leavitt, Lisa Lucas, and Kimberly Olver

ARL-MR-393

December 1998

The findings in this report are not to be construed as an official Department of the Army position unless so designated by other authorized documents.

Citation of manufacturer's or trade names does not constitute an official endorsement or approval of the use thereof.

Destroy this report when it is no longer needed. Do not return it to the originator.

Army Research Laboratory

Adelphi, MD 20783-1197

ARL-MR-393 **December 1998**

Comparison of MBT and BTQB Quantum Well Infrared Photodetectors and Implications for Multicolor Design

Stephen W. Kennerly

Sensors and Electron Devices Directorate, ARL

Daniel W. Beekman, John W. Little, and Arnold C. Goldberg

University of Maryland

Richard P. Leavitt

Sensors and Electron Devices Directorate, ARL

Lisa Lucas and Kimberly Olver

University of Maryland

Abstract

A comparison is presented between two GaAs/AlGaAs quantum well infrared photodetector (QWIP) designs: the miniband transport (MBT) and the bound-to-quasibound (BTQB). Two QWIP test arrays were prepared, designed to have the same peak operating wavelength, doping density, barrier thickness, and excited state binding energy. The detectors are long wavelength infrared (LWIR), each having about a 9.1-μm-peak wavelength. The detector array test structures used edge coupling to remove the grating or optical coupling structure effects from the detector response characteristics. Extensive bias and spectral-dependent blackbody response and specific detectivity data will be presented. The data show that MBT and BTQB QWIPs offer comparable performance.

Contents

Figures

1. Introduction

There has been a substantial amount of interest in the physics and performance of quantum well infrared photodetectors (QWIPs) for several years.[1] The high-quality imagery produced with the use of QWIP focal plane arrays (FPAs) has been impressive,[2] and the design and performance of a single pixel QWIP has been the subject of much interest. The U.S. Army Research Laboratory (ARL), with its Advanced Sensors Consortium Federated Laboratory partners, Lockheed Martin Sanders Corporation and the University of New Mexico, is investigating the use of QWIP FPAs as part of the Multi-Domain Smart Sensors (MDSS) effort. MDSS is expected to offer multispectral infrared (IR) imagery as part of its final demonstration. Various QWIP designs are being considered for implementation into the IR focal plane array to be used in this demonstration. QWIPs from the GaAs/AlGaAs (III-V) material system offer the promise of affordable, large-area format-detector arrays. The QWIP design parameter space is substantial, but the GaAs/AlGaAs material system allows one to reproducibly grow and fabricate devices just as they were initially designed, thus allowing one to steadily improve the detector's performance by optimizing the parameters in the detector design. One of the critical parameters one can optimize is the design of the barriers separating the absorbing quantum wells. In this report, we compare two GaAs/AlGaAs QWIP designs: the miniband transport (MBT) and the bound-to-quasibound (BTQB). In this comparison, we have tried to design, grow, and fabricate two device structures that are identical except for the type of barrier separating the quantum wells. The width of the barrier separating the quantum wells is the same for each structure.

2. QWIP Design

Numerous QWIP designs can yield devices that respond in the infrared. Two QWIP designs that have demonstrated excellent imaging performance are the BTQB[3] and MBT.[4] For both designs, GaAs is used for the quantum well and either AlGaAs or GaAs/AlGaAs is used in their barriers. The two structures differ in the type of barrier separating the wells. The BTQB structure contains continuous AlGaAs barriers with a constant aluminum mole fraction. The MBT structure uses a GaAs/AlGaAs superlattice (SL) barrier. We compared these two structures to

[1]B. F. Levine, K. K. Choi, C. G. Bethea, J. Walker, and R. J. Malik, Appl. Phys. Lett., **50**, 1092 (1987).

[2]W. A. Beck, J. W. Little, A. C. Goldberg, and T. S. Faska, "LWIR Imaging Performance of Miniband Transport Multiple Quantum Well Infrared Focal Plane Arrays," 1993 Meeting of the IRIS Specialty Group on Infrared Detectors, Bedford, MA (17–19 August 1993), p 161.

[3]S. D. Gunapala, J. K. Liu, M. Sundaram, S. V. Bandara, V. Sumith, C. A. Shott, T. Hoelter, P. D. Maker, and R. E. Muller, "Long-Wavelength 256 × 256 QWIP Handheld Camera," Proc. SPIE, Infrared Detectors and Focal Plane Arays IV, **2746**, Orlando, FL (1996), p 124.

[4]W. A. Beck, T. S. Faska, J. W. Little, A. C. Goldberg, J. Albritton, and M. Sensiper, "256 × 256 Focal Plane Array Using Miniband Transport Multiple Quantum Well Infrared Photodetectors," Proc. the Electrochemical Society, 188th Meeting, Chicago, IL (8–13 October 1995).

produce two detector test arrays, each having the same peak response wavelength, excited state binding energy, number of wells, two-dimensional doping density in the quantum well, and barrier thickness separating the absorbing quantum wells. Unfortunately, owing to a miscommunication, the two structures were grown having the same three-dimensional doping density. Since the quantum wells are different widths, this leads to a difference in the (more fundamental) two-dimensional doping density. The effects of this difference in two-dimensional doping are accounted for in our analysis.

Figure 1 shows energy band diagrams for both detector designs at zero field and 5 kV/cm. We calculated the electronic states using Airy function solutions to the Schrodinger equation for the quantum well structures in a uniform electric field. (We will present the details of the calculation, including the treatment of band nonparabolicity, in another paper at a later date.) As the detector is designed, the difference between the ground state and the excited state energies is 137.8 meV, giving a peak absorption wavelength of 9.0 μm. The excited state binding energy (difference between the excited state and the conducting channel) is 12 meV for both designs. This binding energy deviates slightly from the BTQB design of Faska et al,[4] which had the excited state at the top of the barrier (i.e., a zero binding energy).

For the BTQB design (fig. 1, left side), these energies are obtained for a 51–Å GaAs quantum well and an $Al_{0.22}Ga_{0.78}As$ barrier. The MBT design (fig. 1, right side) uses 61-Å GaAs quantum wells, with an SL barrier made of alternating layers of 34 Å of $Al_{0.30}Ga_{0.70}As$ and 11-Å GaAs wells (10 periods plus an additional 34-Å $Al_{0.30}Ga_{0.70}As$ layer). The total barrier thickness for both structures was 484 Å. The detector design consists of 50 quantum wells uniformly doped with silicon to a doping level of $4 \times 10^{17}/cm^3$, separated by the 484-Å barriers. Doped contact layers above and below the 50-quantum well stack have a doping density of $1 \times 10^{18}/cm^3$.

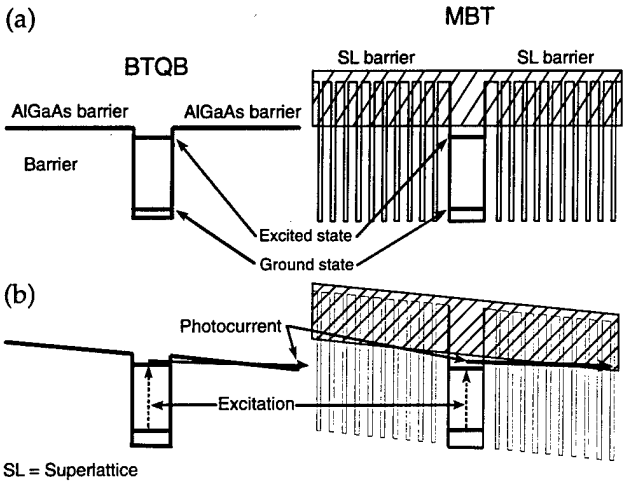

Figure 1. Energy band diagrams of bound-to-quasibound (BTQB) (left) and miniband transport (MBT) (right) QWIPs at (a) zero field and (b) 5 kV/cm.

[4]W. A. Beck, T. S. Faska, J. W. Little, A. C. Goldberg, J. Albritton, and M. Sensiper, "256 × 256 Focal Plane Array Using Miniband Transport Multiple Quantum Well Infrared Photodetectors," Proc. the Electrochemical Society, 188th Meeting, Chicago, IL (8–13 October 1995).

3. Experimental Approach

The GaAs/AlGaAs QWIPs used in this study exhibit the usual polarization sensitivity. When these devices are used for imaging, they always include an optical coupling structure, such as a grating, to facilitate the scattering of the incoming photons, so an electric field component has the required polarization. Optical coupling structures can be sharply peaked in their spectral efficiencies. In QWIPs fabricated with these optical coupling structures, the measured detector response information is actually the convolution of the optical coupling structure with that of the quantum well. To avoid the effects of the coupling structure, we compared the two QWIP designs using detector test structures that are edge coupled. Figure 2 is a diagram of a typical test structure configuration. Although this test structure would not be used as an imaging detector, it does provide good data for this comparison and the optimization effort. It has the additional advantage of being relatively easy to fabricate and mount in cryogenic Dewars for measurements.

Our two test structures were prepared from wafers with the same thickness. The 45° edges were polished with a precision polisher so that both the angle and the distance from the edge to the first row of detector elements would be the same. The opposite edges were formed by cleaving the wafer, with each sample having the same distance from the edge to the detector elements. A highly reflective gold (Au) turning mirror was placed so that its bottom edge vertically aligned with the top edge of the GaAs wafer. (Fig. 2 does not show this alignment.) We attached the detector array chip to a 68-pin leadless ceramic chip carrier (LCC) using conductive epoxy. We subsequently found that the epoxy we used had a small but measurable effect on the spectral response of these structures. Since the effect is small and the same for both structures, it did not affect our comparison.

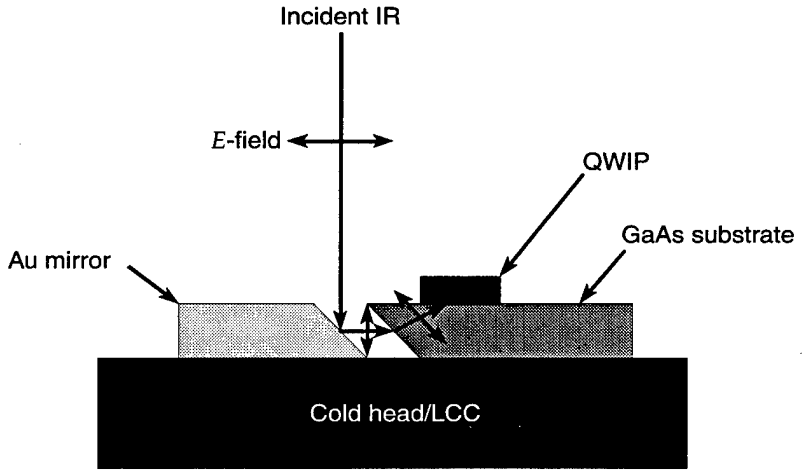

Figure 2. IR detector optical coupling configuration showing 45° edges and Au turning mirror.

It is difficult to account for all the scattered radiation within the GaAs wafer. In an imaging FPA, the substrates for QWIP detector arrays used are thinned so that virtually no scattering in the wafer would lead to cross talk between the elements. In the test structures, however, photons passing through the quantum well stack, but not absorbed, can be totally internally reflected and could be absorbed by other elements in the array. (Of course, this test geometry has no effect on the dark current, only the magnitude of the photoresponse.) The GaAs/AlGaAs wafers had 8×8 arrays of detectors fabricated on them. The square detector elements are 100 μm on a side. For our performance comparison, we used the first row of detector elements: light that is normally incident to the LCC should be reflected by the turning mirror onto the 45° facet and then be refracted onto this first row (see fig. 2). Since both the MBT and BTQB detector test structures have the same geometry, the amount of scattered radiation reaching equivalent pixels is similar.

4. Detector Characteristics

Figure 3 shows the spectral response for each device, measured at –2.0 V. The peak absorption wavelength was designed to be 9.0 μm; in the figure, the MBT device shows a peak response at 9.1 μm, while the BTQB device peaked at 9.3 μm corresponding to a difference in transition energy of 3 meV. The model we used to calculate the energy levels has been developed predominantly with GaAs/AlGaAs MBT structures. The model is being modified to improve accuracy for both MBT and BTQB designs (for example, using a slightly different combination of conduction band offsets and nonparabolicity parameters). The measured peak wavelengths (fig. 3) are similar enough to allow for a meaningful comparison.

Note that both spectral response curves show dips or shoulders on the short wavelength side of the peak and at the same wavelengths. These spectral structures are not systematic of our response measurement system but rather they are due to absorption by the silver epoxy used to mount the devices to the LCC. Evidently, there is significant evanescent

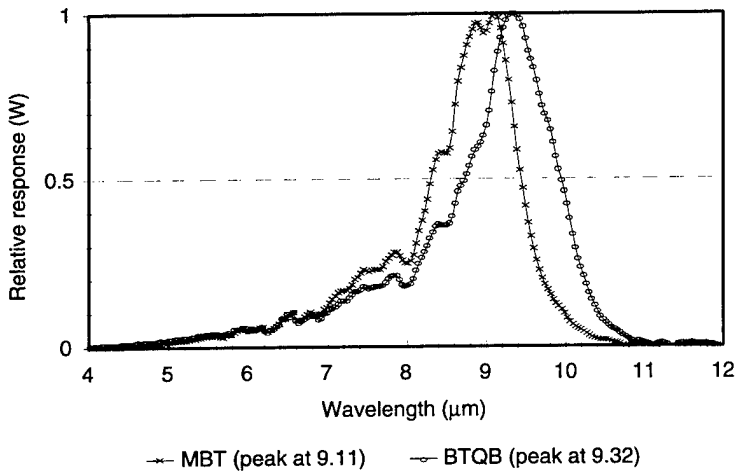

Figure 3. BTQB and MBT QWIP spectral responses taken at –2.0 V.

field coupling of light that is totally internally reflected within the GaAs wafer to the silver epoxy. The strength of the epoxy absorption indicates the presence of scattered light reaching the first row of detector elements. Similar spectral features have been seen in detectors from hybridized fanout test arrays that have epoxy between the GaAs wafer and the fanout chip. Various epoxies can have absorption peaks at different energies. This spectral response structure was not observed in another 8×8 array from the same MBT wafer that had been mounted with indium rather than epoxy. In the spectral data in figure 3, a dip in the detector response spectra appears at 8.97 μm, which is caused by an epoxy absorption line. Without this dip, the MBT detector would peak response close to the design wavelength of 9.0 μm.

Figure 4 gives the 500-K chopped blackbody (BB) responsivity for the two detector designs. The BTQB structure exhibits a broadband response that is 40 percent greater than that of the MBT structure at the usual operating biases, even though the two-dimensional doping density is less. The response for both structures increases monotonically with bias, reaching a maximum of around 3.5 V in each direction. Neither is quite symmetric around zero bias. The response of the BTQB structure diminishes slightly at higher fields.

The most pronounced difference between the MBT and BTQB structures occurs in their photoconductive gains. The photoconductive gains are determined from the noise and current-voltage measurements (under f/3, 295-K background illumination) using the relation

$$g = \frac{\left\langle i_{\text{noise}}^2 \right\rangle}{4qI_{DC}\Delta f},$$

where i_{noise}= current noise, q = charge on an electron, I_{DC} = current, and Δf = noise measurement bandwidth. The current-voltage data for the two structures are shown in figure 5. The bias dependence of the photoconductive gains is shown in figure 6. The gain for the BTQB detector is substantially larger than for the MBT and is responsible for the higher

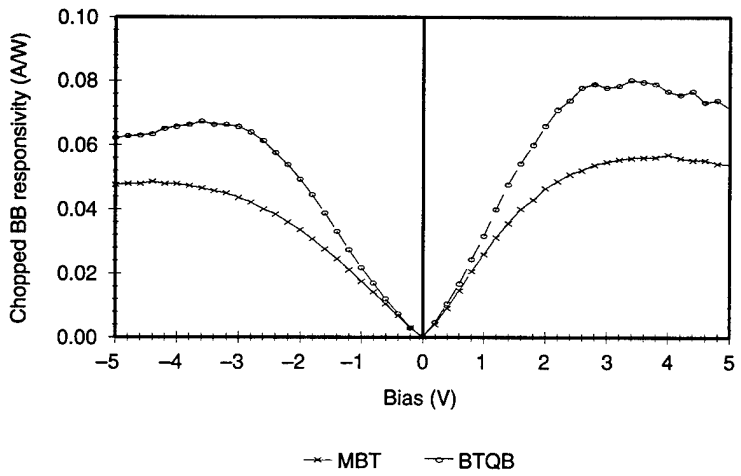

Figure 4. Bias dependence of chopped 500-K responsivity for BTQB and MBT structures at 78 K.

responsivity observed in the BTQB detector. The lower photoconductive gains observed in the MBT device are presumably due to the wider quantum wells and a lower drift velocity in the superlattice, both of which result in the carrier spending more time in the region where capture can occur (i.e., in the doped quantum well). Photoconductive gains in the BTQB structure are approximately twice that of the MBT at reasonable operating biases, much greater than the 20 percent expected from the wider quantum well. The remaining difference is probably due to a lower drift velocity in the SL barrier.[5] We plan to determine the drift velocities for both structures using magneto-transport measurements in another report at a later date.

Peak responsivities can be determined from the spectral response (shown in fig. 3) and the BB responsivities (shown in fig. 4). Using the peak responsivities, peak wavelengths, and the photoconductive gains (shown

Figure 5. Current-voltage data for MBT and BTQB taken at 78 K.

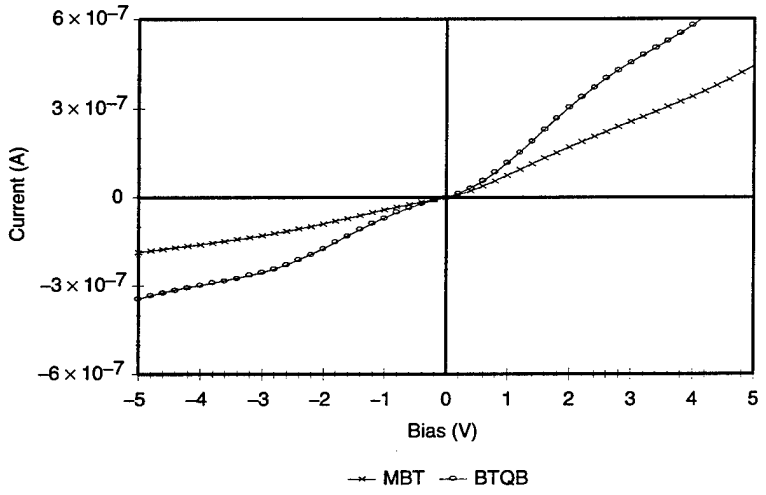

Figure 6. Bias dependence of photoconductive gain for BTQB and MBT structures at 78 K.

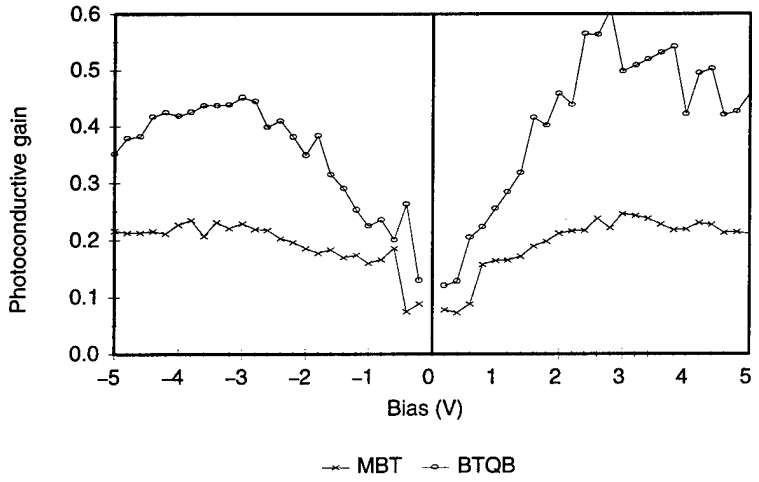

[5]A. C. Goldberg, "Measurement of Electron Transport Properties of GaAs/AlGaAs Superlattice Minibands Populated by Intersubband Transitions in a Quantum Well Infrared Photodetector," Ph.D. dissertation, University of Maryland (1996).

in fig. 6), we derived the absorption quantum efficiencies shown in figure 7. Even though the MBT structure has a lower chopped BB responsivity, it shows a peak absorption quantum efficiency that is approximately 50 percent higher than the BTQB over the typical range of operating biases. The peak absorption quantum efficiency is proportional to the transition probability from the ground state to the first excited state and the two-dimensional doping density. Our model indicates that the transition probability for the MBT structure is about 4 percent greater than the BTQB structure. Higher transition probabilities and two-dimensional doping account for only half the observed difference. Further study will be required to resolve this issue.

The higher response of the BTQB structure might lead one to conclude that it is the better IR detector. However, the structure with the higher response does not necessarily give the better signal-to-noise ratio. Figure 8, showing the chopped 500-K BB detectivities for the two structures, reveals that the MBT has approximately 35 percent higher

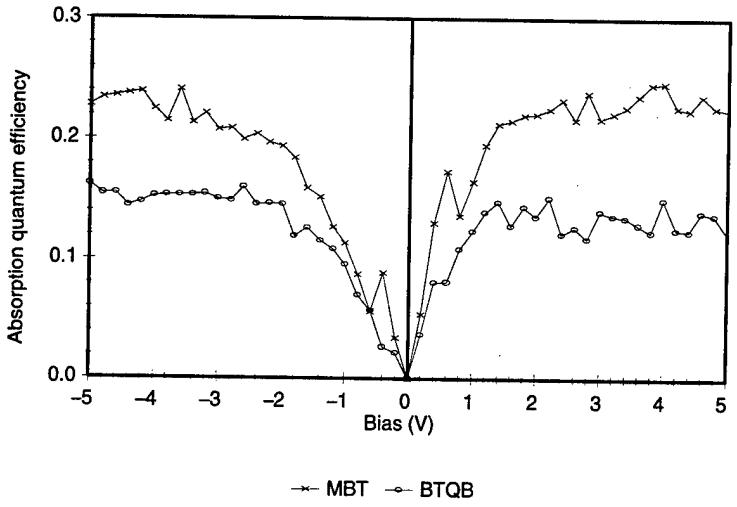

Figure 7. Bias dependence of absorption quantum efficiencies for BTQB and MBT structures at 78 K.

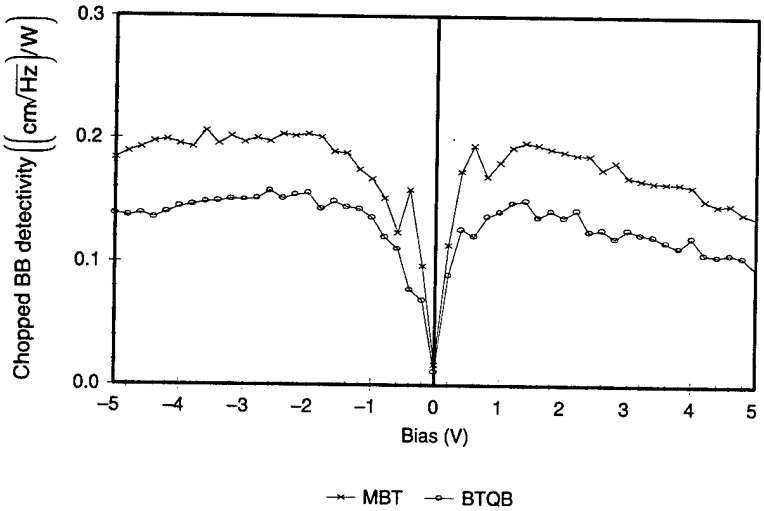

Figure 8. Bias dependence of 500-K chopped BB detectivity for BTQB and MBT structures at 78 K, f/3, 295-K background field of view.

broadband over the entire bias range and thus offers a better signal-to-noise-ratio detector. Of course, the detectivity of the BTQB detector was expected to be slightly lower because of its lower two-dimensional doping and lower activation energy for the dark currents. However, even if we account for these differences, the MBT structure still has about a 10 percent higher broadband detectivity. This difference is probably within the limits of the accuracy of the optical test configuration.

5. Summary

One of the goals of our group is to optimize the QWIP design to produce IR detectors with higher performance and/or operating temperature. The comparison between the BTQB and the MBT detectors presented in this report represents only a single point in a large parameter space available for the design of the structures. Both detectors were designed to have a peak operating wavelength of 9.0 μm with an excited state binding energy of 12 meV, a doping density of $4 \times 10^{17}/\text{cm}^3$, and barrier widths of 484 Å. The spectral shape of the response was very similar for the two structures, but the measured peak wavelength was slightly longer than the design peak for the BTQB. The dark current for the BTQB was about a factor of 2 higher than for the MBT at all biases, which may be due in a large part to the longer cutoff wavelength (see fig. 3).

The most dramatic difference between the two detectors is the photoconductive gain, which is about a factor of 2 higher for the BTQB than for the MBT. This higher gain results in a larger responsivity for the BTQB detector, since the signal is proportional to the gain. On the other hand, the detector shot noise is proportional to the square root of the gain (at 80 K, where the noise generated by dark current dominates). The specific detectivity was higher for the MBT structure, but at least some of the difference could be accounted for by higher dark currents because of the longer peak wavelength for the BTQB. When the detector performance is limited by photocurrent generated by the background irradiance (i.e., at lower temperatures), both the signal and the noise depend linearly on the gain. Therefore, under these conditions, the detectivity (D^*) is independent of the gain. (D^* is proportional to the square root of the absorption quantum efficiency.) The higher quantum efficiency observed for the MBT implies a higher background-limited detectivity.

The additional design flexibility that the MBT structure offers is a substantial advantage over the BTQB. In the BTQB structure, there is only one combination of well width and barrier height (and, therefore, one barrier composition for III-V ternary barriers such as AlGaAs or InAlAs) that produces a specific peak wavelength and excited state binding energy. The use of an MBT SL barrier in which one can vary the position of the bottom of the miniband (i.e., the effective barrier height) over a large range by simply changing the thicknesses of the SL layers (which can be done with high accuracy using molecular beam epitaxy) adds an additional degree of freedom. This additional freedom can be beneficial

for designing more complex structures, such as multicolor QWIP detectors. An example of such a structure is shown in figure 9. In this QWIP structure, which was grown as part of the ARL Federated Laboratory program, we have fabricated a two-color midwavelength infrared/long wavelength infrared (MWIR/LWIR) QWIP for which we used InGaAs/InAlAs lattice matched to an InP substrate to get a well deep enough for MWIR operation. Since well and barrier compositions are fixed by the lattice-matching condition, the only variable of the QWIP is the thickness of the layers. We used a BTQB design to obtain a 4-μm-peak detector for the MWIR section. The BTQB structure has a comparatively higher responsivity at the expense of higher dark current. Because a multicolor detector's operating temperature is limited by the temperature of the LWIR detector, the dark current contribution from the MWIR BTQB portion is insignificant. The InAlAs barrier is much too high in this system to obtain LWIR operation with a BTQB design, but an MBT design allows us to drop the effective barrier (i.e., the miniband) enough to have a 9-μm-peak wavelength detector section grown on top of the MWIR detector section, changing only the layer thicknesses. Using an MBT for the LWIR detection gives the design the same signal-to-noise ratio detection (i.e., D^*) at the long wavelengths but at a comparatively reduced dark current, thus allowing the detector to operate at a higher temperature. Many next-generation QWIP designs involve varying the height of the barrier to imitate built-in internal fields. Since complex barrier designs are relatively easy to obtain with superlattices, this technology offers promise for multispectral IR FPAs.

We are extending our comparison of these two detector structures to cover more of the parameter space. We are currently evaluating a series of MBT and BTQB structures in which the excited state binding energy is varied from 16 to 4 meV in 4-meV steps. We will also include bound-to-continuum designs in which the excited state is above the barrier and compare them with equivalent MBT designs. The results of these tests will be given in a subsequent report.

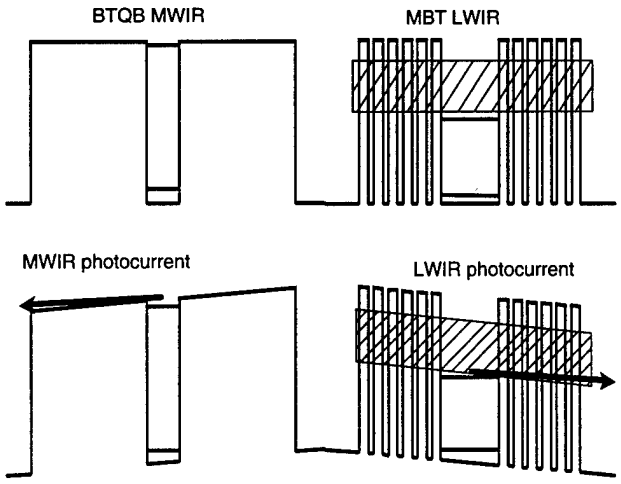

Figure 9. Energy band diagram of an MWIR/LWIR QWIP structure giving two color detections. This structure uses relative advantages of each detector design.

Distribution

Admnstr
Attn Defns Techl Info Ctr
DTIC-OCP
8725 John J Kingman Rd Ste 0944
FT Belvoir VA 22060-6218

Dept of Defns
Attn R222 J Fitz
4800 Savage Rd
FT Meade MD 20755-6000

Ofc of the Dir Rsrch and Engrg
Attn R Menz
Pentagon Rm 3E1089
Washington DC 20301-3080

Ofc of the Secy of Defns
Attn ODDRE (R&AT)
Attn ODDRE (R&AT) S Gontarek
The Pentagon
Washington DC 20301-3080

Ofc of the Secy of Defns
Attn OUSD (A&T)/ODDR&E(R) R Trew
Washington DC 20301-7100

AMCOM MRDEC
Attn AMSMI-RD W C McCorkle
Redstone Arsenal AL 35898-5240

CECOM
Attn PM GPS COL S Young
FT Monmouth NJ 07703

Dir for MANPRINT
Ofc of the Deputy Chief of Staff for Prsnnl
Attn J Hiller
The Pentagon Rm 2C733
Washington DC 20301-0300

Hdqtrs Dept of the Army
Attn DAMO-FDT D Schmidt
400 Army Pentagon Rm 3C514
Washington DC 20301-0460

US Army ARDEC
Attn AMSTA-FSF-RE B95 N H A Jenkinson
Picatinny Arsenal NJ 07806-5000

US Army CECOM
Attn AMSEL-RD-ST-ST-TE L A Coryell
FT Monmouth NJ 07703-5000

US Army Edgewood RDEC
Attn SCBRD-TD J Vervier
Aberdeen Proving Ground MD 21010-5423

US Army Info Sys Engrg Cmnd
Attn ASQB-OTD F Jenia
FT Huachuca AZ 85613-5300

US Army Mis Cmnd
Attn AMSMI-RD-WS-PO J L Johnson
Huntsville AL 35898

US Army Mis Cmnd Weapons Sci Dirctrt
Attn AMSMI-RD-WS-ST M J Bloemer
Redstone Arsenal AL 35898-5358

US Army Natick RDEC
Acting Techl Dir
Attn SSCNC-T P Brandler
Natick MA 01760-5002

US Army Rsrch Ofc
Attn H Everitt
Attn J Harvey
Attn M Dutta
Attn M Stroscio
Attn J Zavada
PO Box 12211
Research Triangle Park NC 27709-2211

US Army Simulation, Train, & Instrmntn Cmnd
Attn J Stahl
12350 Research Parkway
Orlando FL 32826-3726

Distribution (cont'd)

US Army Tank-Automtv & Armaments Cmnd
Attn AMSTA-AR-TD M Fisette
Bldg 1
Picatinny Arsenal NJ 07806-5000

US Army Tank-Automtv Cmnd Rsrch, Dev, & Engrg Ctr
Attn AMSTA-TA J Chapin
Warren MI 48397-5000

US Army Test & Eval Cmnd
Attn R G Pollard III
Aberdeen Proving Ground MD 21005-5055

US Army Train & Doctrine Cmnd Battle Lab Integration & Techl Dirctrt
Attn ATCD-B J A Klevecz
FT Monroe VA 23651-5850

US Military Academy
Dept of Mathematical Sci
Attn MAJ M D Phillips
West Point NY 10996

Nav Surface Warfare Ctr
Attn Code B07 J Pennella
17320 Dahlgren Rd Bldg 1470 Rm 1101
Dahlgren VA 22448-5100

DARPA
Attn B Kaspar
3701 N Fairfax Dr
Arlington VA 22203-1714

Univ of MD Elect Engrg
Attn A Christou
Attn C Davis
Attn M Dagenais
College Park MD 20742

Univ of MD Elect Engrg Dept
Attn R Chen
Baltimore County
Catonsville MD 21228

University of Texas ARL Electromag Group
Attn Campus Mail Code F0250 A Tucker
Austin TX 78713-8029

Hicks & Associates, Inc
Attn G Singley III
1710 Goodrich Dr Ste 1300
McLean VA 22102

Palisades Inst for Rsrch Svc Inc
Attn E Carr
1745 Jefferson Davis Hwy Ste 500
Arlington VA 22202-3402

Inst for Microstructural Sci Natl Rsrch Council of Canada
Attn E Koteles
Attn H C Liu
Building 23 A Montreal Rd
Ottawa Ontario K1A OR6
Canada

NIST
Attn J Comas
Gaithersburg MD 20899

US Army Rsrch Lab
Attn AMSRL-CI-LL Techl Lib (3 copies)
Attn AMSRL-CS-AL-TA Mail & Records Mgmt
Attn AMSRL-CS-EA-TP Techl Pub (3 copies)
Attn AMSRL-SE D Wilmot
Attn AMSRL-SE J Mait
Attn AMSRL-SE J Pellegrino
Attn AMSRL-SE-E H Pollehn
Attn AMSRL-SE-EE B Beck
Attn AMSRL-SE-EE D Beekman
Attn AMSRL-SE-EE Z G Sztankay
Attn AMSRL-SE-EI W Clark
Attn AMSRL-SE-EM A Goldberg
Attn AMSRL-SE-EM D Wortman
Attn AMSRL-SE-EM G Simonis
Attn AMSRL-SE-EM J Little

Distribution (cont'd)

US Army Rsrch Lab (cont'd)
Attn AMSRL-SE-EM K K Choi
Attn AMSRL-SE-EM K Ritter
Attn AMSRL-SE-EM L Lucas (2 copies)
Attn AMSRL-SE-EM R Leavitt (2 copies)
Attn AMSRL-SE-EM K Olver (2 copies)
Attn AMSRL-SE-EM J Little (2 copies)
Attn AMSRL-SE-EE S Kennerly (10 copies)

REPORT DOCUMENTATION PAGE

Form Approved OMB No. 0704-0188

1. AGENCY USE ONLY *(Leave blank)*	2. REPORT DATE	3. REPORT TYPE AND DATES COVERED
	December 1998	Final, 1 Oct 1996–30 Sept 1997

4. TITLE AND SUBTITLE Comparison of MBT and BTQB Quantum Well Infrared Photodetectors and Implications for Multicolor Design

5. FUNDING NUMBERS

DA PR: A31B

PE: 61102A

6. AUTHOR(S) S. W. Kennerly (ARL), D. W. Beekman, J. W. Little, A. C. Goldberg (University of Maryland), R. P. Leavitt (ARL), L. Lucas, K. Olver (University of Maryland)

7. PERFORMING ORGANIZATION NAME(S) AND ADDRESS(ES)

U.S. Army Research Laboratory
Attn: AMSRL-SE-EE email: skennerly@arl.mil
2800 Powder Mill Road
Adelphi, MD 20783-1197

8. PERFORMING ORGANIZATION REPORT NUMBER

ARL-MR-393

9. SPONSORING/MONITORING AGENCY NAME(S) AND ADDRESS(ES)

U.S. Army Research Laboratory
2800 Powder Mill Road
Adelphi, MD 20783-1197

10. SPONSORING/MONITORING AGENCY REPORT NUMBER

11. SUPPLEMENTARY NOTES

ARL PR: 8NE1CC
AMS code: 611102.31B

12a. DISTRIBUTION/AVAILABILITY STATEMENT Approved for public release; distribution unlimited.

12b. DISTRIBUTION CODE

13. ABSTRACT *(Maximum 200 words)*

A comparison is presented between two GaAs/AlGaAs quantum well infrared photodetector (QWIP) designs: the miniband transport (MBT) and the bound-to-quasibound (BTQB). Two QWIP test arrays were prepared, designed to have the same peak operating wavelength, doping density, barrier thickness, and excited state binding energy. The detectors are long wavelength infrared (LWIR), each having about a 9.1-μm-peak wavelength. The detector array test structures used edge coupling to remove the grating or optical coupling structure effects from the detector response characteristics. Extensive bias and spectral-dependent blackbody response and specific detectivity data will be presented. The data show that MBT and BTQB QWIPs offer comparable performance.

14. SUBJECT TERMS	15. NUMBER OF PAGES
QWIP, IR, detector, FPA, GaAs	19
	16. PRICE CODE

17. SECURITY CLASSIFICATION OF REPORT	18. SECURITY CLASSIFICATION OF THIS PAGE	19. SECURITY CLASSIFICATION OF ABSTRACT	20. LIMITATION OF ABSTRACT
Unclassified	Unclassified	Unclassified	SAR

NSN 7540-01-280-5500

Standard Form 298 (Rev. 2-89)
Prescribed by ANSI Std. Z39-18
298-102